INFLUENCE OF MICROSTRUCTURE ON THOUGHNESS OF AN AUSTEMPERED DUCTILE IRON.

(*)J. ARANZABAL, (**) I. GUTIERREZ, J.M. RODRIGUEZ-IBABE AND J.J. URCOLA

ABSTRACT. High Si content in nodular cast iron provides a large amount of retained austenite during isothermal transformation in the bainitic zone. The existence of γ phase gives the material a high toughness with an optimum of $K_{IC} \simeq$ 85 MPa$\sqrt{m}$ for $\sigma_{0,2\%}$ = 1000 MPa at 30% retained austenite. For short time transformation the presence of coarse carbides highly impair the toughness. For lower bainite with austenite volume fractions lower than 30%, the fracture is predominantly transgranular ductile for the optimum in fracture toughness. For austenite volume fraction higher than 30% in the upper bainite region, the $\gamma \rightarrow \alpha'$(martensite) transformation induced plasticity takes place giving the material superior toughness than in conventional cast irons.

INTRODUCTION

Production of bainitic structures by isothermal transformation of austenite (austempering) results in ductile irons having a fairly attractive combination of mechanical properties: high strength (ultimate tensile strength (UTS) of 1000-1500 MN m^{-2}) with acceptable ductility (2-15% elongation), toughness (60-90 MN $m^{-3/2}$), and wear resistance. Thus, the use of austempered ductile irons (ADI) for structural applications has increased greatly and several reviews have recently been published which report new applications such as crankshafts, mining car wheels, and gears (1-4). In most of these applications ADI provides an economical substitute for high strength steels.

In the present study, the influence of the microstructure obtained after various austempering treatments on fracture toughness, has been investigated. Special emphasis has been placed on correlating the amount of retained austenite and its mechanically induced transformation in fracture mechanisms.

(*) INASMET, Camino de Portuetxe, 12, 20009 San Sebastián, Basque Country (SPAIN)
(**) CEIT, P° Manuel de Lardizábal, 15, 20009 San Sebastián, Basque Country (SPAIN)

EXPERIMENTAL

The chemical composition of the ductile iron used in the present work is given in Table 1.

Table 1 Chemical composition of austempered ductile iron (wt-%)

C	Si	Mn	P	S	Mo	Ni	Cu	Ti	Mg
3.69	2.53	0.25	0.014	0.009	0.10	1.07	0.47	0.021	0.045

The austempering heat treatments were carried out by austenitizing for 30 min at 900°C in a chloride salt bath and transforming the austenite isothermally at temperatures in the range 300-410°C for times between 5 min and 24 h in a nitride salt bath.

Standard preparation techniques were used and samples were etched in 4% nital for optical metallography. Thin foil preparation for transmission electron microscopy (TEM) observation was carried out by (i) mechanical polishing, (ii) dimpling of the central zone of the 3 mm discs and (iii) ion milling until perforation. Short rod fracture toughness tests were carried out on specimens of diameter 12 mm (Fig. 1).

RESULTS

After transformation at 300ºC, retained austenite occurs mainly as interlath films, Fig.2, which have a typical wavy morphology characteristic of the bainite formed in high silicon steels, for the lower transformation temperatures (5). The austenite volume fraction is maximum at this temperature for a treatment of 120min and reaches a value of 20%. The measured carbon content of this austenite is 1.7 wt%. Treatments at 370 and 410ºC during 120 min lead to an increase in retained austenite content with volume fraction values of 37 and 45 %,respectively. In this case, the austenite remaining after partial transformation to bainite apart of separating the ferrite plates from each other is also present as large pools of blocky forms, Fig.3. This is a typical morphology of the bainite formed in high silicon steels for this range of temperatures (5). In addition,this austenite is less stable than that produced at 300ºC with carbon contents of 1.6 and 1.4 wt%, for both temperatures, respectively.Shorter treatment times produce a more unstable austenite which transform in martensite on quenching for the entire range of temperatures. At 300ºC the structure remains nearly constant for longer treatment times, on the opposite at the higher temperatures, the austenite decomposes to ferrite and carbides during the isothermal transformation. The rate of austenite decomposition increases with increasing austempering temperature, being nearly complete after 1440min at 410ºC.

The different microstructures generated depending on temperature and time of transformation, show the way through which the heat treatments will affect the

mechanical properties, and particularly the toughness. In Fig.4, fracture toughness values are shown as a funtion of initial retained austenite volume fraction, γ. As γ increases from about 10 to 25%, K_{IC} increases from 20 to 85MN $m^{-3/2}$, but for $\gamma > 25\%$ a saturation is observed and the K_{IC}value is independant of γ. Some data ($K_{IC} < 35$MN $m^{-3/2}$)can not be correlated in terms of γ content with the rest of the results. These data correspond to the shorter treatment times, for wich martensite was present in the microstructure, and to the longest treatment times at 410ºC, for which decomposition of the austenite occurred.

The beneficial effect of retained austenite on toughness, at least for small amounts of austenite, has been associated to different mechanisms (6): a) blunting effect when the crack reaches the ductile austenitic phase, b)crack branching and c) transformation induced plasticity. Mechanisms a) and b) can explain the material behaviour for lowest temperature treatments ($\%\gamma < 25$) due to the stability of the austenite and its distribution (interlath films and isolated pools). In addition,no transformation of the austenite in martensite, induced by deformation has been observed. The fracture mechanisms are transgranular quasicleavage until K_{IC} reaches values close to 60MN $m^{-3/2}$, Fig. 4. For higher values of K_{IC}, the fracture mechanisms is predominantly transgranular ductile and dimples and debonded nodules with high local plastic deformation are present. Showing that at this stage the softer phase controls the deformation mode and the increase in toughness with higher amounts of austenite is related to its ability to deform plastically, rather than to transform.

Variations in austenite content between 30 and ~50% did not result in significant differences in K_{IC} values and the beneficial influence of γ phase on toughness reaches a saturation level. Similar behaviour has been reported for Fe-C -Cr steels (7) and tool steels (8). The fracture mechanisms are a mixture of ductile quasicleavage and intergranular, Fig. 4. The transition at about 30% from a monotonic increase of K_{IC} with γ to an austenite independent region for different materials must be associated to the austenite distribution in the material. In the present case the evolution of bainite formation during austempering treatment may be represented by the sheme in Fig. 5. Bainite forms around the graphite nodules which act as nucleation sites for the bainitic reaction. If the transformation is interrupted in the early stages, the remaining austenite transforms to martensite on cooling but if the treatment time is long enough the bainitic regions can be represented by spheres with their center at nodules, growing until they meet each other. If the reaction is interrupted at this stage, in addition to interlath austenite films triangular isolated γ pools can be found as those found at the lower temperatures. But if the temperature is high, the carbon is able to travel over large distances increasing austenite carbon content and in consequence its stability and the bainitic reaction is interrupted leaving large interconnected pools. This type of microstructure has been observed at 370 and mainly at 410ºC . The transition between these two situations may be modelised by the moment when the spheres

of bainite become tangent. The distribution of nucleation sites (graphite nodule centers) may be described as an array of N_V points per unit volume, separated each other a distance λ and the bainite fraction, f_V, (ferrite + interlath γ films) may be written as:

$$f_V = N_V \times 4/3 \times \pi \times R^3 \qquad (1)$$

where R is the radius of bainitic sphere. The tangency arrises when $2R=\lambda$ and the corresponding volumetric bainite fraction is $f_V= 0.74$. This means that for retained austenite contents higher than about 26% (this value does not take into acount interlath γ films) austenite pools are interconnected and a potential crack propagating into the material will be able to travel all the time into the softer phase. At this moment, the toughness of the material will be independent of austenite volume fraction. This simple model describes correctely the shape of the curve shown in Fig. 4 and explains why different materials exhibit this same behaviour (7, 8, 9). At this stage the austenite controls completely the mechanical response of the material, and in the present case it is stable enough to transform to martensite by plastic deformation (Fig. 6) giving K_{IC} good values. But if the carbon content of the retained austenite is low and in consequence this one is quite unstable, this may cause its transformation to martensite induced by stress (10). In this case, the transformation begins before yield stress is reached causing a dramatic embritlement with the consequent fall in toughness. This kind of behaviour has been previously reported in the litterature by Sandvik and Nevalaiven (11) in a low alloy bainitic austenitic steel which shows a monotonic increase of the impact energy as the γ content increases until about 23% followed by a rapid decrease for higher austenite contents.

REFERENCES

1. J. Dodd: Mod. Cast., May 1978, 60-66

2. J. Vuorinen: "On the strain hardening of austempered spheroidal graphite cast iron", Diss. 48F, Technical Research Centre of Finland, Espoo, Finland, 1981.

3. B.V. Kovacs: J. Heat Treat., 1987, **5**, 55-60.

4. G. Barbezat and H. Mayer: Sulzer Tech. Rev., 1986, (2), 32-38.

5. B.P.J. Sandvik Metall. Trans. A, vol 13A, 1982, pp. 777-787.

6. B.V.N. Rao and G. Thomas: Metall. Trans., 1980, **11A**, 441-457.

7. M. Sarikaya, B.G. Steinberg, and G. Thomas: Metall. Trans., 1982, **13A**, 2227-2237.

8. V. Martínez, R. Palma, and J.J. Urcola: J. Mater. Sci., 1990, **25**, 3359-3367.

9. H.K.D.H. Bhadeshia and D.V. Edmonds: Met. Sci., vol 17, 1983, pp. 411-419.

10. I. Tamura, Met., Sic., vol 16, 1982, pp. 245-253.

11. B.P.J. Sandvik and H.P. Nevalainen: Metals Tech., 1981, pp. 213-220.

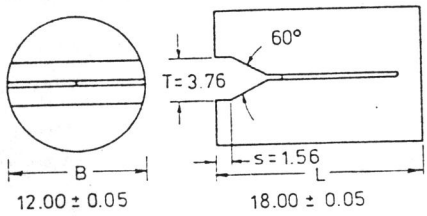

Fig.1 Short rod test specimen (dimensions in mm)

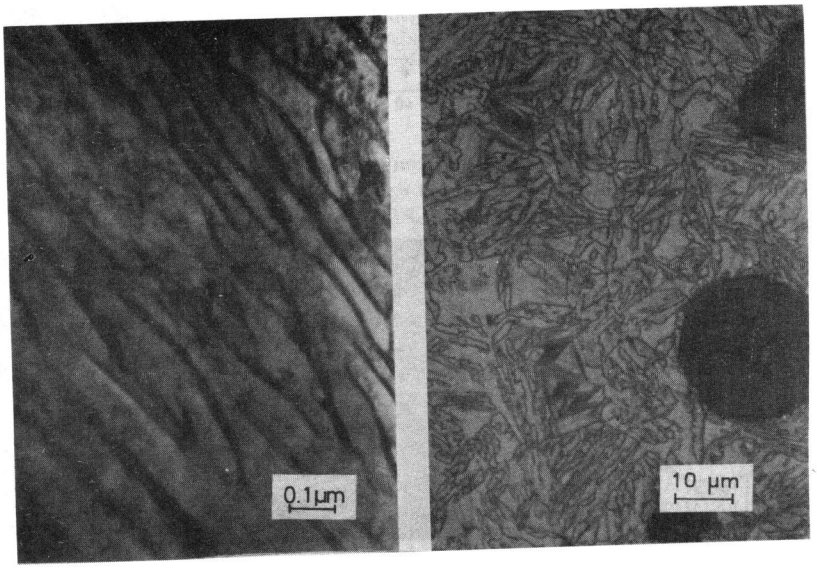

Fig.2 Bainitic structure after an isothermal transformation treatment of 60 min at 300ºC (TEM)

Fig.3 Bainitic structure after an isothermal transformation treatment of 120 min at 410ºC (optical).

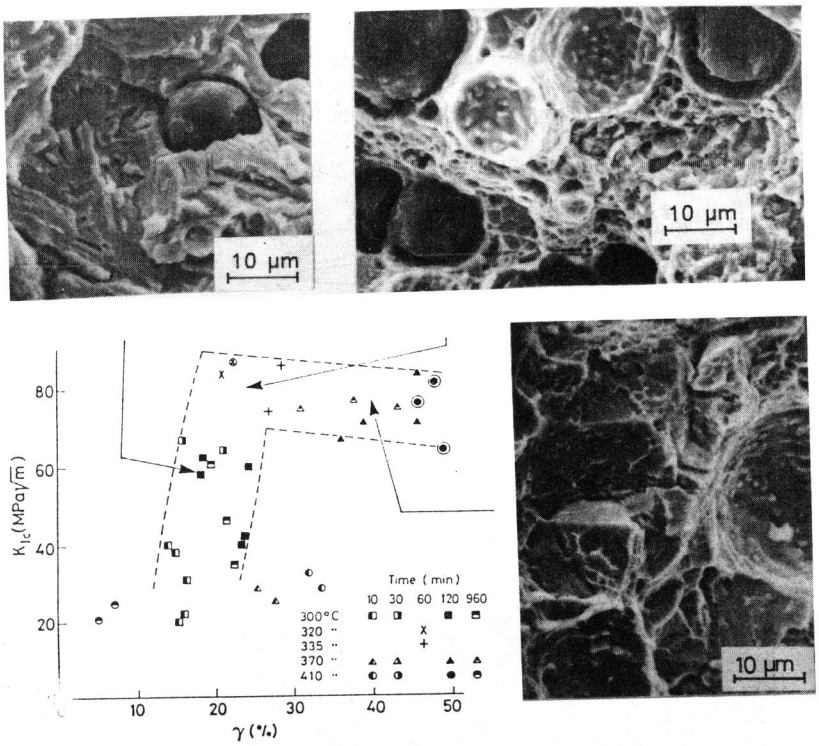

Fig.4 Effect of retained austenite content on K_{Ic}: circled points correspond to conditions for which LEFM was not valid. The fractographs of Barker specimens show various fracture mechanisms (SEM)

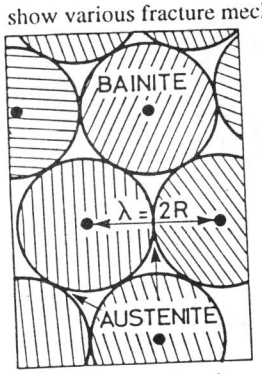

Fig.5 Sheme showing the progress of bainitic reaction.

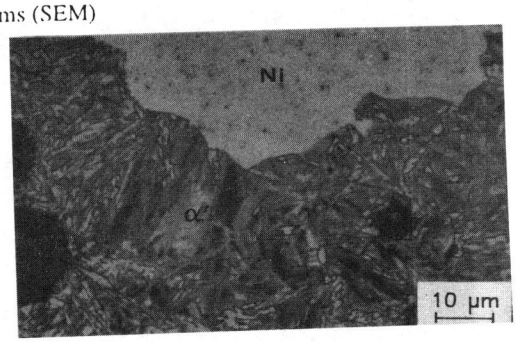

Fig.6 Longitudinal section normal to crack plane of fractured Barker specimen (410ºC/2h) showing martensite induced by deformation.